Rapid communication

High-cycle fatigue behavior of Zn–22% Al alloy processed by high-pressure torsion

In-Chul Choi [a], Byung-Gil Yoo [b], Oliver Kraft [b], Ruth Schwaiger [b], Moo-Young Seok [a], Megumi Kawasaki [a,*], Terence G. Langdon [c,d], Jae-il Jang [a,*]

[a] Division of Materials Science and Engineering, Hanyang University, Seoul 133-791, South Korea
[b] Institute for Applied Materials, Karlsruhe Institute of Technology, Karlsruhe 76021, Germany
[c] Departments of Aerospace & Mechanical Engineering and Materials Science, University of Southern California, Los Angeles, CA 90089-1453, USA
[d] Materials Research Group, Faculty of Engineering and the Environment, University of Southampton, Southampton SO17 1BJ, UK

ARTICLE INFO

ABSTRACT

A Zn–22% Al eutectoid alloy was processed by high-pressure torsion (HPT) and its high-cycle fatigue behavior was explored using novel small-scale bending fatigue experiments. Testing of the finest grain region in each HPT disk showed that the fatigue life decreases continuously with increasing numbers of torsional revolutions. The results are discussed in terms of the HPT-induced hardness change and the underlying fatigue failure mechanism.

© 2014 Elsevier B.V. All rights reserved.

1. Introduction

The Zn–22 wt% Al eutectoid alloy is widely used for damping/energy-absorbing components [1,2] and is well known to exhibit excellent superplastic properties under optimum combinations of temperature and strain rate [3–5]. Recently, there have been efforts to enhance the superplastic properties of the Zn–Al alloy by refining the grains using severe plastic deformation (SPD) techniques [6,7] including equal-channel angular pressing (ECAP) [8] and high-pressure torsion (HPT) [9]. Among the available SPD techniques, HPT processing may be more attractive than ECAP since it is a simpler technique, it can impose higher plastic strains and hence it provides a capability of producing smaller grain sizes [10]. During HPT, the equivalent von Mises strain, ε_{eq}, imposed on the disk is given by [11,12]:

$$\varepsilon_{eq} = \frac{2\pi Nr}{h\sqrt{3}} \tag{1}$$

where r and h are the radius and thickness of the disk and N is the number of torsional revolutions. Thus, the strain varies locally across the disk and is a maximum near the edge.

Recently, extensive research was conducted to investigate the evolution of microstructure and quasi-static mechanical properties (such as hardness and strain-rate sensitivity) of the Zn–22Al alloy during HPT processing [13–16]. However, there was no attempt to monitor the change in the dynamic mechanical properties under cyclic loading of the alloy after HPT processing although such properties are indispensable for practical engineering applications [1,2]. In fact, only limited attention has been given to the fatigue behavior of ultrafine-grained and nanocrystalline metals. In the small number of publications on this topic (see a recent review by Padilla and Boyce [17]), it was reported that the fatigue resistance of metals having a submicrometer grain size can be largely enhanced, which was explained within the framework of a Hall–Petch grain size dependent behavior. In the case of the Zn–22Al alloy, only low-cyclic fatigue testing was reported for the alloy processed by ECAP where the measurements used round-bar specimens under uniaxial loading conditions [1,2]. It should be noted that, while conventional fatigue testing methods are applicable to materials after ECAP having relatively large volumes with homogeneous microstructures, the disk samples produced by HPT are inappropriate for conventional measurements due to their small volumes as well as their inhomogeneous microstructures as suggested by Eq. (1). This difficulty may explain the absence of any attempts to examine the change in fatigue properties after HPT processing.

Accordingly, the present study was initiated as a first report to document the evolution of high-cycle fatigue (HCF) behavior in the Zn–Al alloy after HPT processing. In practice, a novel testing

* Corresponding authors.
E-mail addresses: megumi@hanyang.ac.kr (M. Kawasaki), jijang@hanyang.ac.kr (J.-i. Jang).

system for small-scale bending fatigue was used for the investigation at the edges of the disks where the highest ε_{eq} is imposed during the processing. This testing method, originally developed for thin film metals deposited on Si cantilever arrays [18], applies fully reversible compression-tension strain to the cantilever specimen (i.e., the fatigue strain ratio $R = \varepsilon_{min}/\varepsilon_{max} = -1$) and thereby it is possible to measure HCF life and related damage in a small volume of the specimen.

2. Experimental

The experiments used a commercial Zn–22 wt% Al eutectoid alloy containing a binary microstructure of Al- and Zn-rich phases. Disk samples with a thickness h of ~1.5 mm and radius r of ~5 mm were carefully polished on both sides to give a final h of ~0.8 mm and then annealed in air at 473 K for 1 h to give an average grain size of ~1.4 μm. The HPT processing was conducted under quasi-constrained conditions [19] at room temperature under a compressive pressure of 6.0 GPa and at a fixed rotational speed of 1 rpm. The disks were processed for totals of 1, 2 or 4 turns and measurements at the edges of the disks showed average grain sizes of ~400, ~370 and ~350 nm, respectively. Details of the microstructural changes were demonstrated in recent reports [13–16]. The distribution of the Vickers hardness across the diameter of each disk was measured with HMV-2 equipment (Shimadzu, Tokyo, Japan) at a peak load of 100 g_f. The initial condition before HPT processing showed a hardness of $Hv \approx 68$.

Fig. 1 shows a schematic of the sample preparation procedure and testing system of the novel fatigue technique. From each HPT disk, a cantilever specimen was machined into a rectangular shape with a width of 0.8 mm, length of 9.6 mm and thickness of 0.8 mm by using electrical discharge machining. Both sides of the cantilever were polished with SiC papers and diamond suspensions and then electropolished to a final thickness of ~100 μm for the removal of the damaged surface layers. The cantilever was fixed to a custom-made Al holder and masses, having total weight of ~850 mg to produce the bending load, were attached on both surfaces of the cantilever.
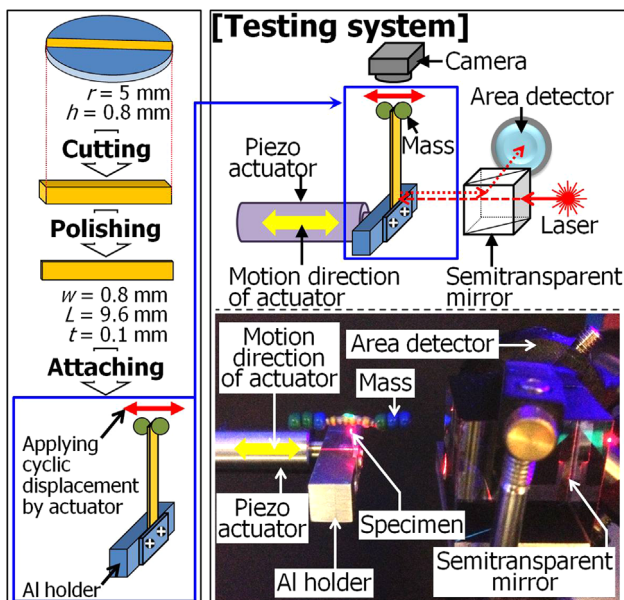
Fatigue testing was performed through a piezoelectric actuator (Physik Instrumente, Waldbronn, Germany) that applied a fully reversible strain by stimulating the beam to vibrate at its resonance frequency. To determine the proper resonance frequency for the cyclic loading, a laser was directed onto the sample and the reflected beam was observed using an area detector (see Fig. 1). Then, the change in the intensity of the reflected laser beam was monitored while the frequency increased, and finally the measured frequency at the maximum intensity was used for the fatigue testing. Other information on the testing system is provided elsewhere [18]. After fatigue testing, the surface damage of the cantilever was analyzed using an ultraviolet laser scanning microscope (UV LSM), VK-9700K (KEYENCE, Osaka, Japan) and the fracture surface morphology was observed with a field-emission scanning electron microscope (FE SEM), Quanta 250 (FEI Inc., Hillsboro, OR).

3. Results and discussion

Fig. 2 shows the variations in Vickers hardness Hv along the radial directions from the centers of the disks after HPT for 1, 2 and 4 turns where the upper dashed line denotes Hv for the unprocessed sample. The Hv values of all processed disks are highest at the centers and decrease with increasing distance from the centers to the peripheries. At the edges, the hardness is almost saturated at points beyond ~2 mm from the centers of the disks. This is in a good agreement with earlier results reporting reasonably homogeneous distributions in hardness and microstructure near the edges of the Zn–22Al disks [13–16]. The results suggest that other mechanical properties may show reasonable consistency when measurements are taken in regions beyond ~2 mm from the center, thereby confirming that the configuration for the fatigue testing shown in Fig. 1 is appropriate for evaluating the fatigue properties (of the edge region with the maximum ε_{eq}) without involving any inherent inhomogeneities of microstructure in the disks after HPT. In Fig. 2, the alloy shows exceptional weakening with increasing ε_{eq} despite significant grain refinement after HPT [13–16] and this is due to a reduction in the rod-shaped Zn precipitates within the Al-rich grains during deformation by HPT [20]. This strain weakening after HPT is characteristic of alloys when processed at high homologous temperatures [21].

In this novel fatigue testing, the fatigue strain amplitude, ε_a, varies along the location of the cantilever and is given as a function of distance from the fixed end, x [22]:

$$\varepsilon_a(x) = \frac{3u_{max}t}{2L^3}(L-x) \qquad (2)$$

Fig. 1. Schematic illustrations of sample preparation procedure and bending fatigue testing set-up.
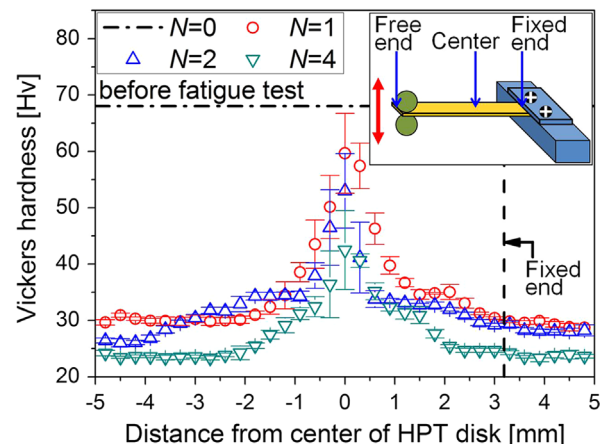

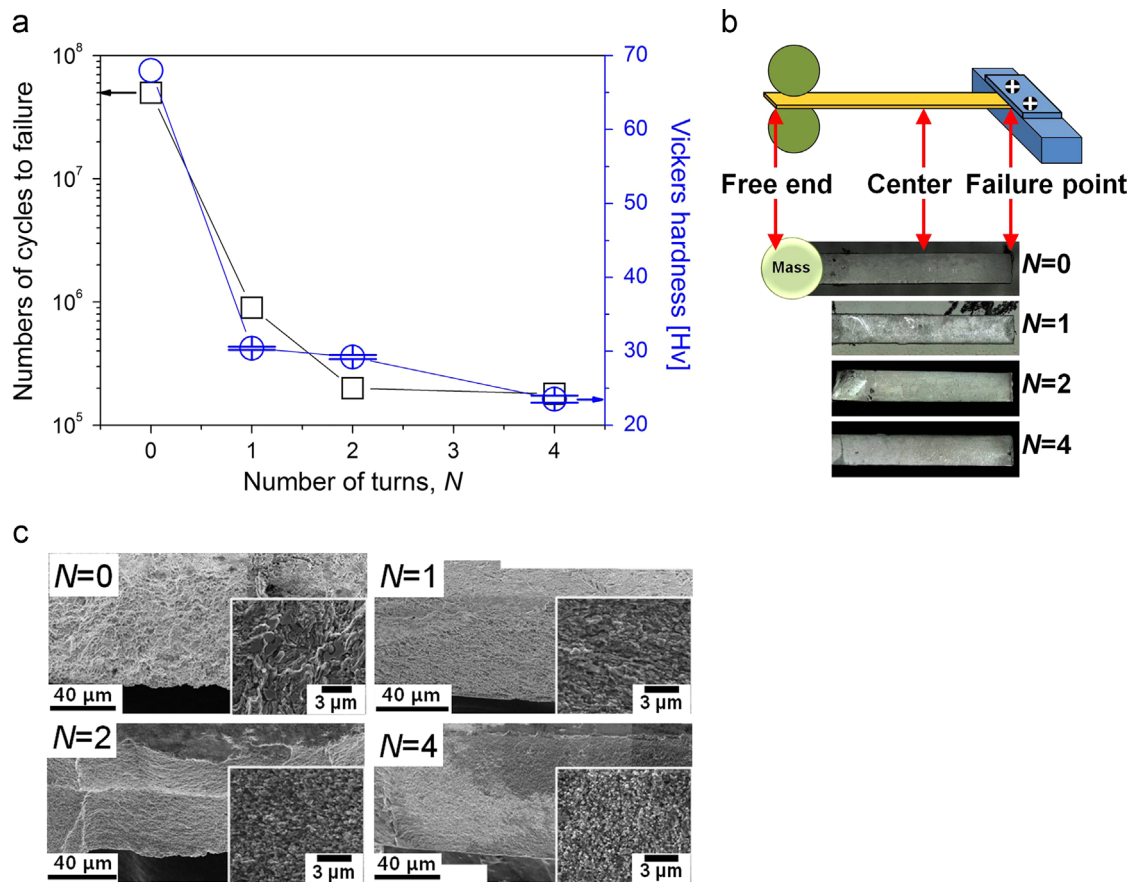**Fig. 2.** Change in Vickers hardness with distance from the center of HPT disk.

Fig. 3. Results of high-cycle bending fatigue tests; (a) changes in fatigue life and Vickers hardness as a function of number of turns; (b) cantilever images taken after fatigue test; (c) SEM micrographs of fracture surfaces at two different scales (note the magnifications of each image are different).

where L and t are the length and thickness of the cantilever, respectively, and u_{max} is the maximum displacement of the cantilever tip. In the present study, the value of u_{max} was directly measured using a digital camera (see Fig. 1) and was observed as about 50 μm for all situations.

The results of the bending fatigue tests are shown in Fig. 3. Fig. 3a summarizes the change in both the numbers of cycles to failure (which is equivalent to the HCF life) and the Vickers hardness at the fixed end in the cantilevers as a function of N. It should be noted that fatigue failure occurred at the fixed end of all cantilevers where ε_a is the maximum (see Fig. 3b). No fatigue damage along the surface of the cantilever was revealed by surface morphology examinations using UV LSM. Moreover, additional Vickers indentation tests (not shown here) demonstrate there is almost no change in the Hv values measured before and after fatigue testing, thereby indicating that there is no damage formation and/or microstructural changes occurring at lower strain amplitudes while the highest stress near the fixed end of the cantilever leads to failure. From the above results, ε_a for the damage-localized fixed end was determined as $\sim 1.23 \times 10^{-4}$ by taking $x=0$ and $u_{max}=50$ μm in Eq. (2).

In Fig. 3a, the estimated HCF life is the highest for $N=0$ with numbers of cycles to failure of $\sim 5 \times 10^7$ and this number decreases with increasing N to $\sim 9 \times 10^5$, $\sim 2 \times 10^5$ and $\sim 1.8 \times 10^5$ for $N=1$, 2 and 4, respectively. This trend is very similar to the change in Hv with increasing N. The reduction in HCF life was supported by fractographic observations as shown in Fig. 3c exhibiting SEM micrographs of the fracture surfaces of the cantilevers at two different scales. An apparent feature is that the tortuosity of the fracture surface is largely reduced as N increases, which implies that fatigue crack propagation of the processed

samples for higher numbers of N tends to occur more easily with less energy needed to create fracture surfaces.

The HCF behavior consists of the two steps of crack initiation and propagation where the former is known to play a much more important role than the latter [23]. In any aspect of crack initiation, the HCF life is governed by the surface strength [24–26]. Specifically, in specimens without notches and other stress concentrators, the crack initiation during HCF occurs typically at surfaces and thus can be significantly resisted by high strength near the surface regions [23]. Thus, the reduction in HCF life with N can be explained by the HPT-induced weakening demonstrated in the hardness measurements as shown in Figs. 2 and 3a. On the other hand, from the viewpoint of crack propagation, the reduction in tortuosity of the fracture surface with increasing N may be closely related to grain refinement irrespective of whether the dominant crack propagation mechanism is intergranular or transgranular [23]. In practice, significant grain refinement reduces the extent of crack tortuosity near the threshold regime where the cyclic plastic zone size is typically smaller than the average grain size. Subsequently, grain refinement leads to a remarkable increase in the crack propagation rate [27] and thus it is reasonable to conclude that the samples after HPT for higher N demonstrate fatigue failure with a higher crack propagation rate that shortens the HCF life. In summary, the Zn–22Al alloy processed by HPT shows a significant reduction in the HCF life and this is in contrast with the general behavior of ultrafine-grained (UFG) materials as, for example, UFG Al where the grain refinement produces an enhancement in both the HCF life and the strength [28]. Nevertheless, in all cases the fractographic observations confirm that the surface strength controls crack initiation and tends to govern the HCF life.

It may be argued that the HCF life of the processed samples is shorter than in the annealed condition because of the significant

Fig. 4. FEA simulations showing strain variations in homogeneous and inhomogeneous cantilevers at a given displacement u_{max}.

gradients in microstructure and hardness along the cantilever. The microstructural gradient may directly affect ε_a but it is not considered in Eq. (2) and thus it is insufficient to directly compare these HCF lives with that of the annealed sample. To address this issue, simple finite-element analysis (FEA) simulations were conducted using ABAQUS (HKS Inc., Pawtucket, RI) software. Two different types of cantilevers, with homogeneous and inhomogeneous strength distributions, were simulated using an eight-node 3D mesh comprised of 768 linear elements. Based on the assumption of an isotropic and an elastic fully-plastic constitutive equation, the free end of the rectangular cantilever having the same geometry as the present experiments was set to have a displacement of $u_{max}=50\ \mu m$. The material parameters used for these simulations were a Young's modulus E of 68 GPa, Poisson's ratio v of 0.3, a density of 5.2 g/cm^3 [29] and yield strengths σ_y which were taken as $\sim H/3$ [30] of 240 and 84 MPa at the highest and lowest values, respectively.

Fig. 4 shows the results of simulations where the simulated bending strain appears in different colors along the cantilevers. In both homogeneous and inhomogeneous cantilevers, the bending strains at the fixed ends show a maximum of $\sim 1.09 \times 10^{-4}$ where this value is consistent with the calculated strain of $\varepsilon_a = 1.23 \times 10^{-4}$ in the present experiments. The influence of inhomogeneity, such as plastic constraints due to neighboring different strengths, was not detected as is evident from the simulated bending strains in both conditions in Fig. 4. Therefore, it is concluded that the gradients of microstructure and strength in the HPT disks have no effect on the HCF life measured at the edges of the disks with the smallest grain sizes.

4. Conclusions

In summary, using a novel small-scale fatigue testing system, the change in high-cycle fatigue behavior was investigated using a Zn–22% Al eutectoid alloy processed by HPT. The fatigue life decreased with increasing numbers of torsional revolutions and this was due to a combination of strain weakening and the significant grain refinement in the alloy through HPT. The validity of the experimental results is supported by finite-element analysis.

Prime novelty statement

– Novel small-scale bending fatigue experiments were conducted to elucidate the high-cycle fatigue (HCF) behavior of Zn–22Al processed by high-pressure torsion (HPT).

– The HCF life decreased with increasing numbers of torsional revolutions due to variation in strength and microstructure during HPT.
– The validity of the experimental results were supported by finite-element analysis.

References

[1] T. Tanaka, M. Kohzu, Y. Takigawa, K. Higashi, Scr. Mater. 52 (2005) 231–236.
[2] T. Tanaka, A. Kushibe, M. Kohzu, Y. Takigawa, K. Higashi, Scr. Mater. 59 (2008) 215–218.
[3] H. Ishikawa, F.A. Mohamed, T.G. Langdon, Philos. Mag. 32 (1975) 1269–1271.
[4] F.A. Mohamed, M.M.I. Ahmed, T.G. Langdon, Metall. Trans. A 8A (1977) 933–938.
[5] A.H. Chokshi, T.G. Langdon, Acta Metall. 37 (1989) 715–723.
[6] M. Kawasaki, T.G. Langdon, Mater. Trans. 49 (2008) 84–89.
[7] M. Kawasaki, T.G. Langdon, Mater. Sci. Eng. A 528 (2011) 6140–6145.
[8] R.Z. Valiev, T.G. Langdon, Prog. Mater. Sci. 51 (2006) 881–981.
[9] A.P. Zhilyaev, T.G. Langdon, Prog. Mater. Sci. 53 (2008) 893–979.
[10] T.G. Langdon, Acta Mater. 61 (2013) 7035–7059.
[11] R.Z. Valiev, Yu.V. Ivanisenko, E.F. Rauch, B. Baudelet, Acta Mater. 44 (1996) 4705–4712.
[12] F. Wetscher, R. Pippan, S. Sturm, F. Kauffmann, C. Scheu, G. Dehm, Metall. Mater. Trans. A 37A (2006) 1963–1968.
[13] M. Kawasaki, B. Ahn, T.G. Langdon, Acta Mater. 58 (2010) 919–930.
[14] M. Kawasaki, B. Ahn, T.G. Langdon, Mater. Sci. Eng. A 527 (2010) 7008–7016.
[15] I.C. Choi, Y.-J. Kim, B. Ahn, M. Kawasaki, T.G. Langdon, J.-i. Jang, Scr. Mater. 75 (2014) 102–105.
[16] T.-S. Cho, H.-J. Lee, B. Ahn, M. Kawasaki, T.G. Langdon, Acta Mater. 72 (2014) 67–79.
[17] H.A. Padilla, B.I. Boyce, Exp. Mech. 50 (2010) 5–23.
[18] S. Burger, C. Eberl, A. Siegel, A. Ludwig, O. Kraft, Sci. Technol. Adv. Mater. 12 (2011) 054202.
[19] R.B. Figueiredo, P.H.R. Pereira, M.T.P. Aguilar, P.R. Cetlin, T.G. Langdon, Acta Mater. 60 (2012) 3190–3198.
[20] M. Furukawa, Z. Horita, M. Nemoto, R.Z. Valiev, T.G. Langdon, J. Mater. Res. 11 (1996) 2128–2130.
[21] M. Kawasaki, J. Mater. Sci. 49 (2014) 18–34.
[22] S. Burger, PhD Dissertation, Karlsruhe Institute of Technology, Karlsruhe, Germany, 2013.
[23] T. Hanlon, E.D. Tabachnikove, S. Suresh, Int. J. Fatigue 27 (2005) 1147–1158.
[24] R.W. Landgraf, ASTM STP 467 (1970) 3–36.
[25] J.D. Morrow, ASTM STP 378 (1965) 45–87.
[26] H. Mughrabi, H.W. Höppel, Mater. Res. Soc. Symp. Proc. 634 (2001) (B2.1.1–B2.1.12).
[27] S. Suresh, Fatigue of Materials, second ed., Cambridge University Press, Cambridge, 1998.
[28] H.W. Höppel, L. May, M. Prell, M. Göken, Int. J. Fatigue 33 (2011) 10–18.
[29] ⟨http://www.matweb.com⟩.
[30] I.-C. Choi, Y.-J. Kim, Y.M. Wang, U. Ramamurty, J.-i. Jang, Acta Mater. 61 (2013) 7313–7323.